

# Synthetic magnetic field effects on neutral bosonic condensates in quasi three-dimensional anisotropic layered structures

T. A. Zaleski

*Institute of Low Temperatures and Structure Research,  
Polish Academy of Sciences, POB 1410, 50-950 Wrocław 2, Poland*

T. P. Polak

*Adam Mickiewicz University of Poznań, Faculty of Physics, Umultowska 85, 61-614 Poznań, Poland*

We discuss a system of dilute Bose gas confined in a layered structure of stacked square lattices (slab geometry). A derived phase diagram reveals a non-monotonic dependence of the ratio of tunneling to on-site repulsion on the artificial magnetic field applied to the system. The effect is reduced when more layers are added, which mimics a two- to quasi-three-dimensional geometry crossover. Furthermore, we establish a correspondence between anisotropic infinite (quasi three-dimensional) and isotropic finite (slab geometry) systems that share exactly the same critical values, which can be an important clue for choosing experimental setups that are less demanding, but still leading to the identical results. Finally, we show that the properties of the ideal Bose gas in a three-dimensional optical lattice can be closely mimicked by finite (slab) systems, when the number of two-dimensional layers is larger than ten for isotropic interactions or even less, when the layers are weakly coupled.

PACS numbers: 05.30.Jp, 03.75.Lm, 03.75.Nt

## I. INTRODUCTION

Systems of dilute bosonic gases confined in optical lattices are ideal toolboxes for testing theoretical models and their solutions [1]. However, investigation of their properties under external magnetic field seemed to be precluded, since the particles used in the experiments are uncharged atoms and thus, are not directly affected by the magnetic field. Fortunately, development of various experimental techniques allow to investigate ultracold systems that are described by exactly the same Hamiltonians as the ones interacting with external magnetic field. Furthermore, they lead to appearance of vortices in Bose-Einstein condensates (BEC), which is a hallmark of a superfluid in a magnetic field. One of those techniques results from equivalence between the Lorentz force and the Coriolis force. As a result, rotation of the condensate (usually rotation of the masks with set of holes located in the laser beams producing quasi-two-dimensional rotating optical lattice) acts as a synthetic magnetic field (SMF) [2–4]. However, this approach puts limit on maximum rotational velocity, thus large SMF (e.g. required for quantum Hall physics) cannot be reached. To overcome those difficulties, imprinting of the quantum mechanical phase is used, which is based on superimposing of an external potential on a BEC (e.g. by applying rotating magnetic field) [5, 6]. Another approaches are stirring a BEC with laser beam [7], or using additional Raman lasers to coherently transfer atoms from one internal state to another. This induces a non-vanishing phase of particles moving along a closed path, which simulates magnetic flux through the lattice [8, 9]. Additionally, rectification of the magnetic field in the optical lattice by using a superlattice allows to ensure that each plaquette

acquires the same phase, thus simulating the uniform magnetic field for any value of phase between 0 and  $\pi$  [10].

A ground state of neutral atoms in an optical trapping potential can be either superfluid (SF) or a Mott-insulator (MI). The zero-temperature coupling ( $t/U$ ) vs. chemical potential ( $\mu/U$ ) phase diagram contains characteristic lobes marking a quantum phase transition between SF and MI states;  $t$  is the matrix element for tunneling between adjacent lattice sites and  $U$  is the on-site energy cost for multiple occupancy. For average number of particles per site equal to one, the transition occurs at the ratio  $(t/U)_{\text{crit}}$ , which is strongly dependent on the geometry of the system. Recently, many very precise calculations and measurements have been performed to obtain correct value of the  $(t/U)_{\text{crit}}$ . For the three-dimensional (3D) optical lattices, most methods converge to  $(t/U)_{\text{crit}}^{3D} = 0.03$  [11, 12], but lower-dimensional cases are more demanding because of growing influence of the quantum fluctuations. In order to precisely describe experimental results, it is necessary to develop a theory that contains fully tunable lattice degrees of freedom, includes effects of the synthetic magnetic field and is non-perturbative, which allow to capture essential physics of strongly correlated system in  $U/t \gg 1$  regime. To this end, we constructed a theoretical field approach, in which the dimensionality along  $c$  axis can be tuned by adding an arbitrary number of single layers along with variable tunneling between them (thus including anisotropy of tunnelling between and within planes). In principle, we can include sixty layers as in the experiments of the Spielman's group [13], or just a few as in the Krüger setup [14], where the magnetic confinement along the  $z$ -direction was used to localize atoms in the effectively  $\mathcal{N} = 4k_B T / m\omega_z^2 l^2 \sim 2 \div 4$  central lattice planes ( $T$  is

the temperature,  $\omega_z$  is the frequency at the bottom of the lattice wells and  $l$  is the lattice period that can be adjusted to any value higher than half of the atomic resonance wavelength). The Burger group [15] developed method in which by increasing the nodal planes of the optical lattice superposed to a 3D potential it is possible to follow the transition from three-dimensional system to an two-dimensional array. Therefore the system becomes quasi-3D rather than purely planar. That can be used in order to look in the interference between planes and in consequence to access to spatial coherence of such structure.

The outline of the paper is as follows: in Sec. II we introduce the model Hamiltonian and the effects of artificial magnetic field and briefly describe our method. In Sec. IV, we present our results starting with the zero-temperature phase diagrams and its dependence on the system geometry. Furthermore, we show the influence of the synthetic magnetic field on properties of the Bose-Hubbard system. Also, we find a correspondence between systems sharing the same critical properties but differing with the geometry of the optical lattice and interactions, which can be a helpful clue on choosing between various experimental setups. Finally, we conclude in Sec. V.

## II. MODEL

In optical lattices, two main energy scales are set by the hopping amplitude  $t$  (the kinetic energy of bosons tunneling between the lattice sites), and the on-site repulsive interaction  $U$  (resulting from repulsion of multiple boson occupying the same lattice site). For  $t \gg U$ , the superfluid order is well established in zero-temperature limit. However, for sufficiently large repulsive energy  $U$ , the quantum phase fluctuations lead to suppression of the long-range phase coherence resulting in SF to MI transition. The critical ratio of  $(t/U)_c$  for which this transition occurs depends strongly on the number of bosons introduced to the optical lattice (which in theoretical models is often controlled by a chemical potential  $\mu$ ). The synthetic magnetic field  $\mathbf{B}$  (resulting either from rotation of the system, phase imprinting, or external electric field) introduces the Peierls phase factor  $e^{\frac{2\pi i}{\Phi_0} \int_{\mathbf{r}_j}^{\mathbf{r}_i} \mathbf{A} \cdot d\mathbf{l}}$ , where  $\mathbf{B} = \nabla \times \mathbf{A}(\mathbf{r})$ , and  $\Phi_0 = hc/e$  is the flux quantum, with  $\mathbf{A}(\mathbf{r})$  being the vector potential (which can be realized experimentally, see Ref. [9]), and  $h$ ,  $c$  and  $e$  – Planck constant, speed of light and charge of electron, respectively. Thus, the system can be described by the following quantum Bose-Hubbard Hamiltonian [16, 17]

$$\mathcal{H} = \frac{U}{2} \sum_{\mathbf{r}} n_{\mathbf{r}} (n_{\mathbf{r}} - 1) - \sum_{\langle \mathbf{r}, \mathbf{r}' \rangle} t_{\mathbf{r}\mathbf{r}'} e^{\frac{2\pi i}{\Phi_0} \int_{\mathbf{r}_j}^{\mathbf{r}_i} \mathbf{A} \cdot d\mathbf{l}} a_{\mathbf{r}}^\dagger a_{\mathbf{r}'} - \mu \sum_{\mathbf{r}} n_{\mathbf{r}}, \quad (1)$$

where  $a_{\mathbf{r}}^\dagger$  and  $a_{\mathbf{r}}$  are for the bosonic creation and annihilation operators that obey canonical commutation relations  $[a_{\mathbf{r}}, a_{\mathbf{r}'}^\dagger] = \delta_{\mathbf{r}\mathbf{r}'}$ ,  $n_{\mathbf{r}} = a_{\mathbf{r}}^\dagger a_{\mathbf{r}}$  is the boson number operator on the site  $\mathbf{r}$ . Here,  $\langle \mathbf{r}, \mathbf{r}' \rangle$  denotes summation over the nearest-neighbor sites. Furthermore,  $t_{\mathbf{r}\mathbf{r}'}$  is the hopping matrix element with the dispersion  $t_{\mathbf{k}} = 2t_{\parallel} \left( \cos k_x + \cos k_y + \frac{t_{\perp}}{t_{\parallel}} \cos k_z \right)$  where  $t_{\perp}$  is the hopping between layers and  $t_{\parallel}$  within the planes. Since, we are interested in investigating the influence of the lattice geometry on the system properties, we consider a stack of an arbitrary number ( $L$ ) of two-dimensional planes coupled with  $t_{\perp}$ . As a result, the values of  $k_x$  and  $k_y$  are continuous ( $k_{x,y} = -\pi, \dots, \pi$ ), while  $k_z$  is discrete ( $k_z = \frac{2\pi}{L}l$ , where  $l = 0, \dots, L-1$ ). Also, we allow for  $c$ -axis anisotropy, which is a ratio of inter-plane to in-plane hopping  $\eta = t_{\perp}/t_{\parallel}$ .

A boson hopping around a lattice cell of the area of  $A$  will gain an additional phase  $2\pi f$  resulting from the synthetic magnetic field, where  $f = ABe/2\pi\hbar$ . As a result, the properties of the system will be periodic with a period corresponding to  $1/f$ . As a result, the periodic potential leads to splitting of Landau levels into integer number  $q$  of sub-bands. Of special interest are the values of the SMF which correspond to rational numbers of  $f \equiv p/q = 1/2, 1/3, 1/4, \dots$  ( $p$  is an integer), since for those values the energy spectra and the density of states can be obtained exactly, although it is analytically feasible only for small values of  $q$ . In the present paper, we present new results for  $f = 1/8$  and  $f = 3/8$ , which up to now have been analytically inaccessible (see, Ref. [18]). Since, all properties of the Hamiltonian Eq. (1) are invariant under  $f \rightarrow -f$  and also under  $f \rightarrow f + 1$ , it is sufficient to consider  $f$  in the range  $0 < f < 1/2$ . In solid state physics obtaining  $f = 1/2$  in experimental setup would require magnetic field of the order of  $10^5 T$ . In optical lattices however, due to larger lattice spacings (and larger  $A$  consequently), much smaller values of  $\mathbf{B}$  of the order of  $10^{-3} T$  are required. This makes investigation of the above-mentioned rational values of  $f$  reasonable.

To proceed, we rely on the quantum rotors approach. The method is extensively described in Refs. [12, 17, 19, 20], so here we only summarize its main points. We use the functional integral representation of the model with bosonic operators becoming complex fields  $a_{\mathbf{r}}(\tau)$  (where  $\tau$  is imaginary Matsubara's time). The most important element of our method is a local gauge transformation to the new bosonic variables:

$$a_i(\tau) = b_i(\tau) \exp[i\phi_i(\tau)]. \quad (2)$$

This allows to cast the strongly correlated bosonic problem into a system of weakly interacting bosons, submersed into the bath of strongly fluctuating gauge potentials on the high energy scale set by  $U$ . It also allows to formulate the problem in the phase representation, which is the best suited to describe MI to SF transition, since it is governed by phase fluctuations. As a result, the superfluid order parameter can be written as:

$$\Psi_B \equiv \langle a_i(\tau) \rangle = b_0 \psi_B, \quad (3)$$

where non-zero value of  $\psi_B = \langle \exp[i\phi_i(\tau)] \rangle$  results from phase ordering and  $b_0$  is the amplitude of the bosonic field:

$$b_0^2 = \left[ 4 + 2 \left( 1 - \frac{1}{L} \right) \frac{t_\perp}{t_\parallel} \right] \frac{t_\parallel}{U} + \frac{\mu}{U} + \frac{1}{2}. \quad (4)$$

The coefficient  $4 + 2 \left( 1 - \frac{1}{L} \right) \frac{t_\perp}{t_\parallel}$  is an effective number of nearest neighbors averaged over all lattice sites. In the zero-temperature limit we arrive at the equation for the phase order parameter:

$$1 - \psi_B^2 = \frac{1}{2N} \sum_{\mathbf{k}} \frac{1}{\sqrt{\frac{J_{\mathbf{k}=0} - J_{\mathbf{k}}}{U} + v^2 \left( \frac{\mu}{U} \right)}} \quad (5)$$

with

$$v \left( \frac{\mu}{U} \right) = \text{frac} \left( \frac{\mu}{U} \right) - \frac{1}{2}, \quad (6)$$

where  $\text{frac}(x) = x - [x]$  is the fractional part of the number and  $[x]$  is the floor function which gives the greatest integer less than or equal to  $x$  and the phase stiffness  $J_{\mathbf{k}} = b_0^2 t_{\mathbf{k}}$ .

Since the number of layers  $L$  in the system is finite, the summation in Eq. 5 runs over discrete values of  $k_z$  and continuous values of  $k_x$  and  $k_y$ . However, because density of states of a single layer under SMF ( $\rho_f$ ) is known, we explicitly derive the density of states of the whole stack of  $L$  coupled planes (for calculation details, see Ref. [21]):

$$\rho_f^L(\eta, \xi) = \frac{1}{L} \sum_{k_z} \rho_f(\xi - \eta \cos k_z). \quad (7)$$

As a result, the critical line equation ( $\psi_B = 0$ ) including the effects of SMF and  $c$ -axis anisotropy reads:

$$1 = \frac{1}{2} \int_{-\infty}^{+\infty} d\xi \frac{\rho_f^L(\eta, \xi)}{\sqrt{2(\xi_0 - \xi) b_0^2 \frac{t_\parallel}{U} + v^2 \left( \frac{\mu}{U} \right)}}, \quad (8)$$

with  $\xi_0$  being the half-width of the band dispersion for selected value of  $f = p/q$ .

### III. RESULTS

#### A. Phase diagram

The Eq. (8) allows us to calculate the zero-temperature phase diagram of the investigated Bose-Hubbard model from Eq. (1) as a dependence of critical interaction on the chemical potential, SMF, number of layers and  $c$ -axis anisotropy:

$$\left( \frac{t_\parallel}{U} \right)_c = x_c = x_f^L \left( \frac{\mu}{U}, \eta \right). \quad (9)$$

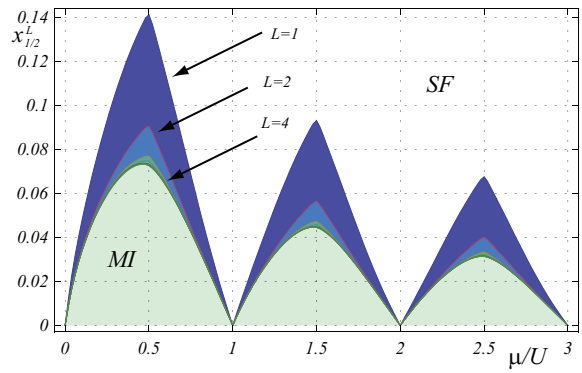


Figure 1: (Color online) The zero-temperature phase diagram of a stack of square lattice planes (number of particles per lattice site is  $n_B = 1$  inside the first and  $n_B = 2$  and 3 in second and third lobe, respectively) with magnetic field  $f = 1/2$  for various number  $L$  of layers and  $\eta = 1$ . Within the MI phase the phase order parameter  $\Psi_B = 0$ .

The diagram is plotted in Fig. 1 for different number of layers  $L$ , synthetic magnetic field  $f = 1/2$ , in isotropic case ( $\eta = 1$ ). In the weak coupling limit ( $t_\parallel \gg U$ ), the kinetic energy dominates and the ground state is a delocalized superfluid, described by nonzero value of the superfluid order parameter  $\Psi_B \neq 0$ . On the other hand, in the strong coupling regime ( $t_\parallel \ll U$ ) the phase fluctuation become significant and the long-range order is destroyed leading to a series of MI lobes with fixed integer filling  $n_B = 1, 2, \dots$  [12, 16]. A single-layer system ( $L = 1$ ) has a simple square (two-dimensional) geometry, which results in the phase diagram with characteristic narrow-edged lobes. As the number of layers is being increased, the tops of the lobes become smooth and their maxima deviate towards lower values of the chemical potential  $\mu$  (this effect is also clearly presented in Ref. [22]). As a result, the phase diagram becomes similar to the one of a cubic (three-dimensional) system. It is important to notice, that also in the presence of the synthetic magnetic field, the phase diagrams of the finite  $L$  system becomes indistinguishable from the infinite (cubic) one for  $L$  as small as 10. For example, for ten layers, the value of  $x_{1/3}^{10}$  is 102.2% of the infinite system  $x_{1/3}^\infty$  and for sixty -  $x_{1/3}^{60}$  is close to 100.1% of  $x_{1/3}^\infty$ . The phase diagram obtained from the quantum rotor approach (QRA) was verified several times [17, 19] by comparison with the very precise numerical methods: quantum Monte-Carlo [11] and diagrammatic perturbation theory [22]. The QRA phase diagrams were also compared to an analytical works: mean-field theory [23] and Padé analysis [24]. From the above, it is expected that QRA accurately captures the low energy physics of the Bose-Hubbard model in the more demanding case where the system is placed under an artificial magnetic field.

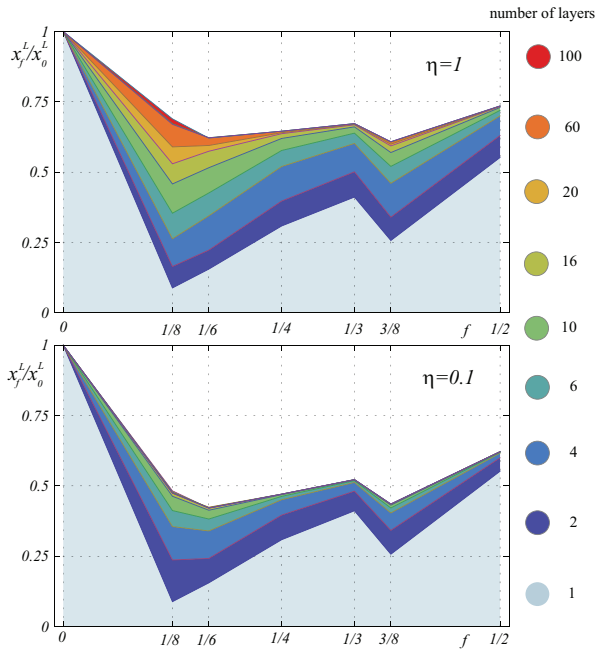


Figure 2: (Color online) Ratio of critical coupling  $x_0^L/x_f^L$  of the tip of the first lobe [see, Eq. (9)] of the system without ( $f = 0$ ) and with synthetic magnetic field  $f$  as a function of number layers  $L$  for isotropic (top)  $\eta = 1$  and anisotropic (bottom)  $\eta = 0.1$  case, respectively.

### B. Effect of the synthetic magnetic field and the system geometry

The transition, experimentally seen in the time-of-flight images (the presence of sharp peaks has been considered as an unequivocal signature of superfluidity in the Bose system), occurs rather rapidly with increasing lattice depth. Because the experimental parameter  $V_0/E_R$  ( $V_0$  is the maximum value of the lattice depth), depends logarithmically on  $U/t$ , the small changes of the dimensionless depth of the optical lattice can cover a wide range of the phase diagram. The phase coherent Bose gas can be also driven into the Mott insulating phase by applying the synthetic magnetic field. The effect of the SMF is presented in Fig. 2. The long range order is suppressed by the phase changes imposed on the bosonic wave function and this suppression has a non-monotonic character strongly depending on the topology of the system. The Mott insulating phase becomes more stable, which is as expected since the magnetic field should localize particles. In the single-layer system, the effect of the SMF is the most pronounced and this decreases with growing number of layers  $L$ . By adding more layers the global coherence of the system is restored, because growing dimensionality entails the suppression of quantum fluctuations effects. Here, the convergence of properties of the finite system to those of the infinite (cubic) one is much slower, although also non-trivially dependent on  $f$  (for some values like  $f = 1/8, 1/6$  and  $3/8$  seems to be much

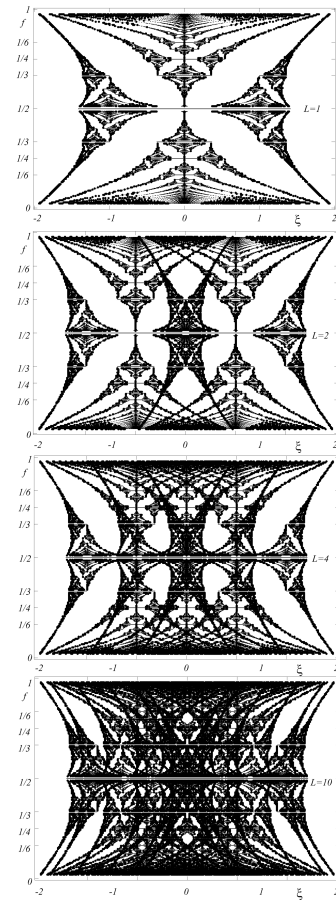


Figure 3: The evolution of the Hofstadter butterfly with increasing number of layers  $L$  in the isotropic case of tunneling ratio  $t_\perp = t_\parallel$ . Adding more layers simply results in additional fractal patterns and very complex structures of  $L$  butterflies emerging.

more pronounced than for  $f = 1/4, 1/3$  and  $1/2$ ). When the system is anisotropic (see, the bottom plot in Fig. 2), the convergence is much faster, but still depending on the specific value of  $f$ .

In the non-interacting ( $U = 0$ ) Bose-Hubbard model under the synthetic magnetic field, the energy spectrum is known as the Hofstadter butterfly [25] (see, the top plot for  $L = 1$  in Fig. 3). The band width is strongly dependent on  $f$  and exhibits a self-similar gap structure for rational values of  $f$ . It has been observed, that in the mean-field approach, the critical hopping  $x_f^1$  roughly follows the bandwidth of the Hofstadter's butterfly [23]. However, in our results the non-monotonicity of  $x_f$  is not exactly following the Hofstadter butterfly bandwidth, especially for lower values of  $f$ . Also, we calculate the band for multiple-layer system and present it in Fig. 3. It is clear, that increasing the number of layers (for  $L > 1$ ) does not influence the width of the band, while the  $x_0^L/x_f^L$  in Fig. 2 evidently changes while converging to the three-dimensional (cubic) case. We would like to note that, both densities of states for square system in the mag-

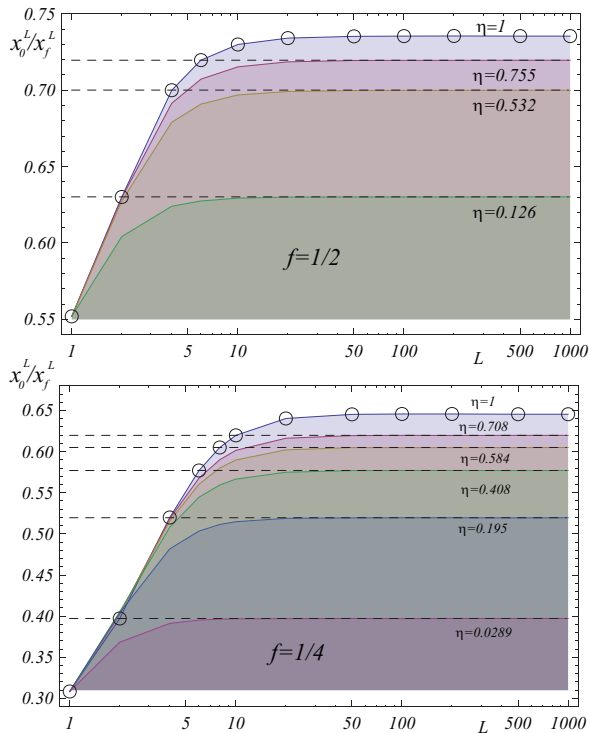


Figure 4: (Color online) The evolution of normalized critical ratio  $x_0^L/x_f^L$  with number of layers for magnetic field  $f = 1/2$  and  $f = 1/4$  with different values of the tunneling ratio  $\eta = t_\perp/t_\parallel$ . Dashed lines show correspondence between systems with finite and infinite  $L$ .

netic field  $\rho_f$  and DOS of  $L$ -layer stack  $\rho_f^L(\eta, \xi)$  are obtained exactly in analytical form with any approximations. The Hofstadter's band structure has also been investigated in context of quantum graphs and the integer quantum Hall effect[26], where similar energy spectra for two-dimensional to three-dimensional system crossover have been observed (non-symmetry of the spectra results from their representation as functions of wave vectors instead of energy).

### C. Correspondence between finite $L$ -layer and infinite systems

Although, conventional optical lattices typically possess a uniform tunneling matrix elements, by changing lasers intensity along  $z$  axis one can control the tunneling between adjacent layers. Sometimes the tunneling rate between adjacent sites is just negligible on the time scale of experiments [14]. On the other hand, using a mask in the novel holographic methods [27] one can also reproduce almost arbitrary potential. Such fully controllable optical environment allows us to restrict the spatial (along  $z$  axis) degree of freedom of the particles and introduce  $c$ -axis anisotropy to the system. In consequence, the tunneling between planes can be different from that

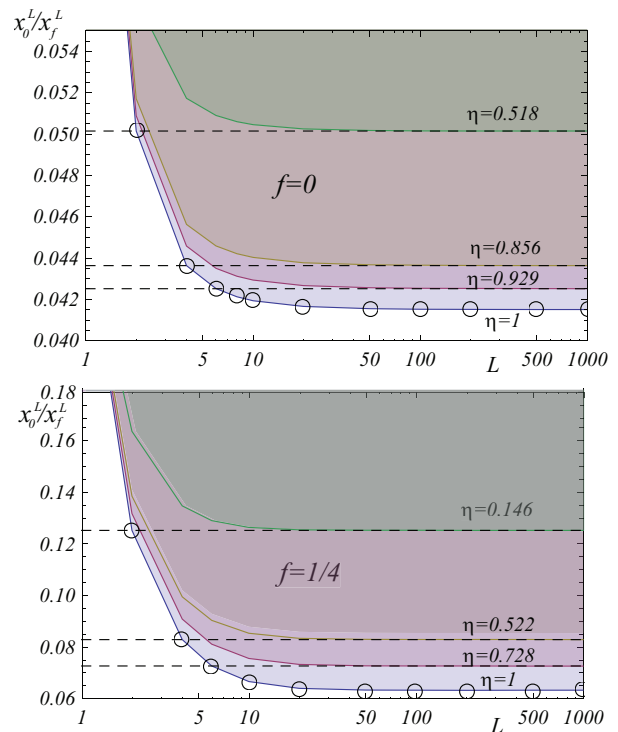


Figure 5: (Color online) The evolution of normalized critical parameter  $x_0^L/x_f^L$  with number of layers without magnetic field and for  $f = 1/4$  with different values of the tunneling ratio  $\eta = t_\perp/t_\parallel$ . Dashed lines show correspondence between systems with finite and infinite  $L$ .

in the single layer  $t_\perp \neq t_\parallel$  or even completely suppressed. However, since some experimental setups can be more convenient to use than others, one can try to establish a correspondence between number of layers and anisotropy, i.e. find values of  $L$  and  $\eta$  that result in the systems that share the same properties in time-of-flight experiments, thus are interchangeable. The results are presented in Figs. 4 and 5 for two setups: when the effect of the field is compared to the system in zero field ( $x_0^L/x_f^L$ , see Fig. 4), and when the bare critical value of  $x_f^L$  is monitored (see, Fig. 5). In both cases, we calculate  $x_0^L/x_f^L$  or  $x_f^L$  as a function of finite number of layers  $L$  for isotropic ( $\eta = 1$ ) system. Then, we determine the anisotropy ratio  $\eta$  for the infinite cubic system ( $L \rightarrow \infty$ ), which results in the same  $x_0^L/x_f^L$  or  $x_f^L$  values. For example, from Fig. 4 it is clear that 4-layer (quasi 2D) isotropic system corresponds to 3D cubic system with anisotropy ratio equal to  $\eta = 0.755$  ( $f = 1/2$ , top plot). If the field value  $f = 1/4$ , a 3D system of similar anisotropy ( $\eta = 0.708$ ) shares the properties with 10-layer isotropic one. Fig. 5 shows, that the  $c$ -axis anisotropy is less important when the magnetic field is turned off (values of  $\eta$  are closer to isotropic  $\eta = 1$  case).

#### IV. CONCLUSIONS

We have calculated critical properties of the layered structure of strongly interacting bosons under a synthetic magnetic field. Derived phase diagram reveals a non-monotonic dependence of the ratio of tunneling to on-site repulsive interaction on artificial magnetic field applied to the system. By calculating analytically the density of states (cases with  $f = 1/8$  and  $f = 3/8$  have not been presented in the literature) for several values of the magnetic field we were able to accurately predict the evolution of the system towards the Mott phase. The effect is reduced when more layers are being added, i.e. during the two- to quasi three-dimensional geometry crossover.

Furthermore, we have established a correspondence between anisotropic infinite (quasi three-dimensional) and isotropic finite (slab geometry) systems that share exactly the same critical values, which can be an important clue for choosing experimental setups that are less demanding, but still leading to the identical results. Finally, we have shown that the properties of the ideal Bose gas in three-dimensional optical lattice can be closely mimicked by finite (slab) systems, when the number of two-dimensional layers is larger than ten or even less, when the layers are weakly coupled.

**Acknowledgments.** T.A.Z. wants to acknowledge that the present work is supported from scientific financial resources in the years 2009-2012 as a research grant.

- 
- [1] D. Jaksch, and P. Zoller, *Ann. Phys.* **315**, 52 (2005).
  - [2] I. Coddington, P. C. Haljan, P. Engels, V. Schweikhard, S. Tung, and E. A. Cornell, *Phys. Rev. A* **70**, 063607 (2004).
  - [3] S. Tung, V. Schweikhard, and E. A. Cornell, *Phys. Rev. Lett.* **97**, 240402 (2006).
  - [4] V. Schweikhard, S. Tung, and E. A. Cornell, *Phys. Rev. Lett.* **99**, 030401 (2007).
  - [5] A. E. Leanhardt, A. Görlitz, A. P. Chikkatur, D. Kielpinski, Y. Shin, D. E. Pritchard, and W. Ketterle, *Phys. Rev. Lett.* **89**, 190403 (2002).
  - [6] Y. Zheng, and J. Javanainen, *Phys. Rev. A* **67**, 035602 (2003).
  - [7] K. W. Madison, F. Chevy, W. Wohlleben, and J. Dalibard, *Phys. Rev. Lett.* **84**, 806 (2000).
  - [8] D. Jaksch, and P. Zoller, *N. Journ. Phys.* **5**, 56 (2003).
  - [9] Y.-J. Lin, R. L. Compton, K. Jiménez-García, J. V. Porto, I. B. Spielman, *Nature*, **462**, 628 (2009).
  - [10] F. Gerbier, and J. Dalibard, *New J. Phys.* **12**, 033007 (2010).
  - [11] B. Capogrosso-Sansone, Ş. G. Söyler, Nikolay Prokof'ev and B. Svistunov, *Phys. Rev. A* **77**, 015602 (2008).
  - [12] T. P. Polak and T. K. Kopeć, *Phys. Rev. B* **76**, 094503 (2007).
  - [13] I. B. Spielman, W. D. Phillips, and J. V. Porto, *Phys. Rev. Lett.* **98**, 080404 (2007).
  - [14] P. Krüger, Z. Hadzibabic, and J. Dalibard, *Phys. Rev. Lett.* **99**, 040402 (2007).
  - [15] S. Burger, F. S. Cataliotti, C. Fort, P. Maddaloni, F. Minardi and M. Inguscio, *Europhys. Lett.* **57**, 1, (2002).
  - [16] M. P. A. Fisher, P. B. Weichman, G. Grinstein, and D. S. Fisher, *Phys. Rev. B* **40**, 546 (1989).
  - [17] T. P. Polak and T. K. Kopeć, *Phys. Rev. B* **79**, 063629 (2009).
  - [18] T. P. Polak, to be published elsewhere.
  - [19] T. P. Polak and T. K. Kopeć, *J. Phys. B* **42**, 095302 (2009).
  - [20] T. K. Kopeć, *Phys. Rev. B* **70**, 054518 (2004).
  - [21] T. A. Zaleski and T. K. Kopeć, *J. Phys. A* **43**, 425303, (2010).
  - [22] N. Teichmann, D. Hinrichs, M. Holthaus, and A. Eckardt, *Phys. Rev. B* **79**, 100503 (2009).
  - [23] M. Ö. Oktel, M. Niță, and B. Tanatar, *Phys. Rev. B* **75**, 045133 (2007).
  - [24] M. Niemeyer, J. K. Freericks, and H. Monien, *Phys. Rev. B* **60**, 2357 (1999).
  - [25] D. R. Hofstadter, *Phys. Rev. B* **14**, 2239 (1976).
  - [26] N. Goldman and P. Gaspard, *Phys. Rev. B* **77**, 024302 (2008).
  - [27] W. S. Bakr, J. I. Gillen, A. Peng, S. Fölling and M. Greiner, *Nature*, **462**, 74 (2009).
  - [28] Y. Hasegawa, P. Lederer, T. M. Rice, and P. B. Wiegmann, *Phys. Rev. Lett.* **63**, 907 (1989).